SEVENTH FRAMEWORK PROGRAMME

CAPACITIES - ERA.Net RUS: Linking Russia to the ERA

Contract for: **Innovation Project**

D.6
Guidelines for Future Missions Data Analysis

Project acronym: **GEOURBAN**
Project full title: Exploitin**G** **E**arth **O**bservation in s**U**stainable u**RB**an pl**A**nning & ma**N**agement
Contract no.: ERA.Net-RUS-033
Date: 25/07/2013

Doc.Ref.: GEOURBAN_35_TR_DLR

Book Captain: M. Marconcini

Contributors: M. Marconcini, T. Esch, H. Taubenböck,

Issue: 2.0

Deliverable no.: D.6
Dissemination: RE

Document Status Sheet

Issue	Date	Author	Comments
1.0	21/07/2013	M. Marconcini T. Esch H. Taubenböck	Draft out for consortium review
2.0	25/07/2013	D. Triantakonstantis N. Chrysoulakis	Final Version

Table of Contents

Background

The beginning of the 21st century represented a historic moment in the development of humankind. At that time, the number of urban residents exceeded the rural population for the first time in history, hence marking the start of an “urban century” (UNDP, 2008). According to the United Nations Development Program (UNDP) almost two-thirds of the world’s population will live in cities by the year 2030. Hence, the lion’s share of the world’s population growth over the next three decades will be concentrated in urban areas (Esch et al., 2012).

New data sources and innovative concepts are needed to even document what is happening in our ever-increasing cities across the world. From a physical point of view, Earth observation (EO) has the unique capability to provide an ever-increasing amount of data sets to capture the physical effects of urbanization. While more and more studies focusing on the EO-capabilities for urban analysis are evolving and new fields of applications are breaking new grounds, current missions and thus currently used EO-data have a certain life time. Thus, this report is giving an overview on planned and proposed missions capable to at least continue existing applications in the urban remote sensing domain, but mostly likely to even improve the capabilities in the next 10 years.

1. Introduction

Urban remote sensing is a relatively new research and application field developing especially since the launch of satellites with very high spatial resolutions (VHR) back in 1999. At present, a large range of sensors is available for urban remote sensing. They differ in spatial and spectral resolution, spatial coverage, temporal revisit capability and data costs. The different characteristics of available data allow very different methodological and thematic developments - from classification algorithms to applications in thematic fields such as urban planning, population assessments, risk analysis. The specific characteristics of urban areas (i.e., their large-scale objects and structural changeovers within few meters) imply certain requirements for EO-data depending on the geoinformation product relevant for the user.

To date, EO-analyses on urbanized areas have been carried out at very different spatial resolutions:

1. At medium spatial resolution (MR), global urban maps are generated by using imagery collected from optical sensors as MODIS (NASA, 2013a), DMSP-OLS (NOAA, 2013a), AVHRR (NOAA, 2013b), MERIS (ESA, 2013a), SPOT-4-VEGETATION (CNES, 2013). In this context, so far MODIS 500 and GlobCover 2009 are the two most accurate settlements layers available worldwide with a spatial resolution of 493 and 309 meters, respectively (Potere et al., 2009).
2. High spatial resolution (HR) data are typically used for regional analyses including thematic characterization of major urban types. In such framework, both optical (e.g., Landsat TM and ETM+ (NASA, 2013b), SPOT (CNES, 2013), IRS LISS and AWiFS (ISRO, 2013), as well as radar sensors (e.g., TerraSAR-X (DLR, 2013a), TanDEM-X (DLR, 2013b), RADARSAT (CSA, 2013), ALOS-PALSAR (JAXA, 2013), Cosmo SkyMed (UGS, 2013) are generally employed with a spatial resolution ranging from 10 to 50 m.
3. Local-scale analyses are carried out by means of very high resolution data (VHR) acquired by optical systems - e.g., RapidEye (RapidEye, 2013), CARTOSAT (ISRO, 2013), IKONOS (DigitalGlobe, 2013), QuickBird (DigitalGlobe, 2013), WorldView 1 and 2 (DigitalGlobe, 2013), GeoEye 1 and 2 (DigitalGlobe, 2013) - or radar satellites such as TerraSAR-X (DLR, 2013a), TanDEM-X (DLR, 2013b), or RADARSAT (CSA, 2013). The spatial resolution up to ~0.4 m allows a fine characterization of urban areas with high spatial detail.
4. Using digital surface models derived from stereo imagery of VHR optical sensors such as CARTOSAT-1 or WorldView II, it became even possible to map complex urban environments in their third dimension. New perspectives with respect to the characterization of building volumes, although at a coarser resolution, are to be expected by the TanDEM-X mission.

So far, a wide variety of methods have been developed to exploit the capabilities of the abovementioned EO missions to tackle urban analyses. In this framework, most relevant applications include urban extent mapping, change detection for urban sprawl analysis, urban structure type characterization, risk and vulnerability assessment, as well as transdisciplinary analyses related to population growth, energy consumption and climate change. For a comprehensive analyses of state-of-the-art methodologies and applications, the reader is referred to the recent special issues on “Urban Remote Sensing” published in the Journal of Remote Sensing in 2011 (Hay & Blaschke, 2011) and on “Remote Sensing of the Urban Environments” published in Remote Sensing of Environment in 2012 (Weng Quattrochi & Carlson, 2012) or to books such as “Urban Remote Sensing: Monitoring, Synthesis and Modeling in the Urban Environment” (Yang, 2011) or “Remote Sensing of Urban and Suburban Areas” (Rashed & Jürgens, 2010).

Future missions will continue the path defined by current missions or even enlarge the capabilities for urban remote sensing to develop and provide key geoinformation products. In this context, most relevant missions include Sentinel 1, 2 and 3 (ESA, 2013b) to be operated by ESA, EnMAP (EnMAP, 2013) to be operated by DLR and HyspIRI (NASA, 2013c) to be operated by NASA. In the following, an overview is presented of relevant future missions grouped according to the different types of sensor they mount on board, i.e. radar, multispectral and hyperspectral.

2. Radar missions

2.1. Sentinel-1

Sentinel-1 is one of the 5 new ESA missions aimed at tackling the operational needs of the European GMES/COPERNICUS programme. Sentinel-1 is a polar-orbiting satellite system dedicated to the continuation of Synthetic Aperture Radar (SAR) operational applications building on ESA’s and Canada’s heritage SAR systems (i.e., ERS-1, ERS-2, Envisat ASAR, Radarsat). The mission will mount a C-band imaging radar sensor which will provide all-weather day-and-night imagery at different spatial resolutions. The first Sentinel-1 satellite is envisaged to be launched in February 2013 and will be followed by the second satellite a few years later. The technical details are presented in Table 1, whereas an artistic impression of the satellite is given in Figure 1.

With respect to the on-going TerraSAR-X (TSX) and TanDEM-X (TDX) missions and the related Global Urban Footprint (GUF) initiative of DLR (Esch et al., 2012), aiming at the global mapping of human settlements in a so far unique spatial detail (see Figure 2), this ESA mission holds high capabilities for continuative urban monitoring. The authors are currently transferring and testing the developed classification technique to different sensors and imaging modes of various SAR systems, including ERS-1 and ERS-2, as well as ASAR, which are the precursors of the Sentinel-1 mission.

Sentinel-1 is a crucial mission in using radar data for continuing applications in the context of a characterization and consistent monitoring of urbanized areas such as already

Table 1: Technical details of Sentinel-1.

Name	**SENTINEL-1 (A&B)**		
System	C-band SAR		
Operator	ESA		
Planned Launch	~ 2013		
Technical details	**Acquisition mode/ Spectral resolution**	*Interferometric Wide Swath*	*Wave*
	Geometric resolution	5*20 m	5*5 m
	Swath	250 km	20 km
	Revisit time	12 days (one satellite) / 6 days (two satellites)	

demonstrated on the basis of ERS-1/2 and ENVISAT-ASAR data by Strozzi et al. (2000), Weydahl (2001), Jiang et al. (2008), or Gamba & Lisini (2012). As shown by Marconcini et al. (2013), the GUF products can be used for large area characterization of urban and rural settlement patterns as well as for improving the long-time monitoring of urban growth or sprawl (Taubenböck et al., 2012a). In the study from Taubenböck et al. (2012a), all mega cities across the globe have been classified, a major task considering the large areas of currently 28 mega cities. The combination with optical Landsat data allows consistent time-series analysis for the analysis of dimension, dynamics and patterns of urbanization processes. As the urban footprint imitative at DLR will provide a global baseline layer for urbanized areas, the Sentinel-1 mission has the capability to continue the monitoring of urban sprawl and urbanization on a global level.

Figure 1. *Artistic impression of Sentinel-1.*

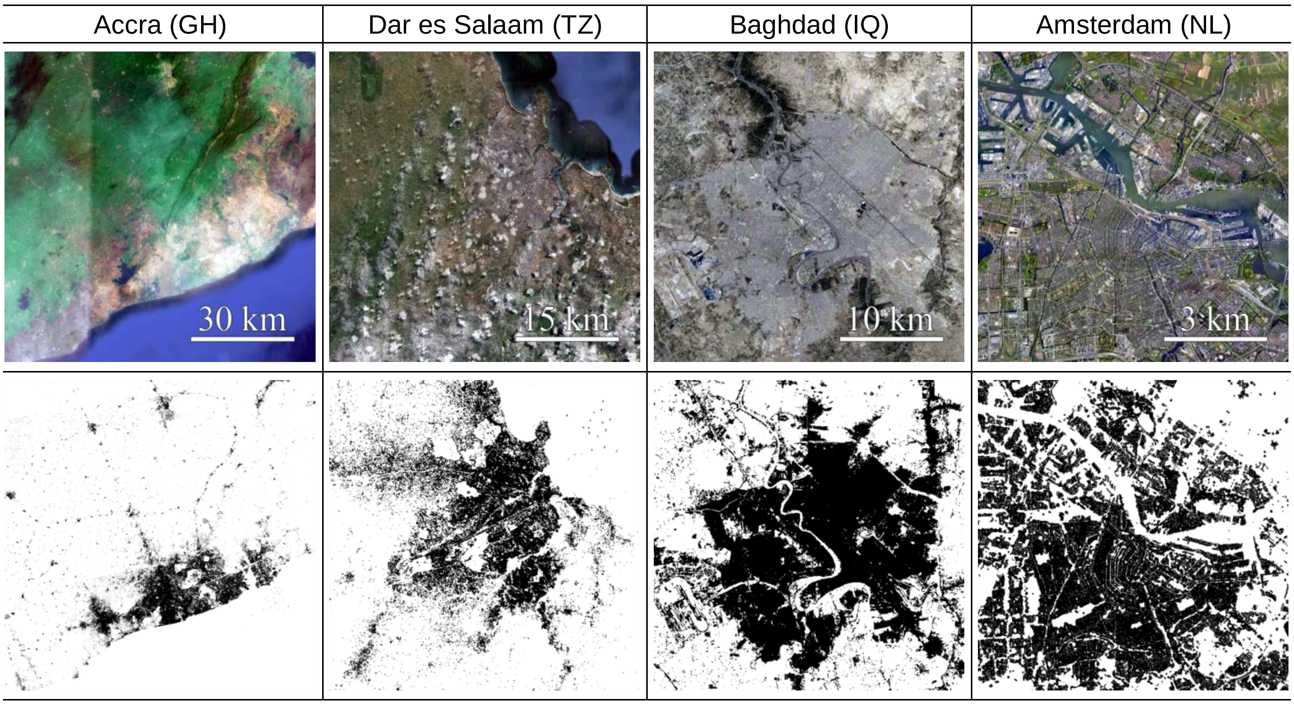

Figure 2. *Optical data (from Google Earth) and corresponding Global Urban footprint for the cities of Accra (GH), Dar es Salaam (TZ), Baghdad (IQ), Amsterdam (NL) (Marconcini et al., 2013).*

2.2. RADARSAT Constellation

The new RADARSAT Constellation is the evolution of the current RADARSAT Programme with the objective of ensuring data continuity, improved operational use of SAR data and improved system reliability. The three-satellite configuration will provide complete coverage of Canada's land and oceans offering an average daily revisit, as well as daily access to 95% of the world to Canadian and International users. The mission development has begun in 2005, with satellite launches planned for 2018 (CSA, 2013). The technical details of the system are presented in Table 2.

The greatly enhanced temporal revisit time combined with accurate orbital control will enable advanced interferometric applications on a four-day cycle that will allow the generation of very accurate change-detection maps. The RADARSAT Constellation mission will ensure C-band data continuity for RADARSAT users, but will also allow a series of novel applications enabled through the constellation approach. The first satellite of the constellation will be launched in the way to ensure no data gap at RADARSAT-2 end of life. The system does not aim to reproduce RADARSAT-2, but rather to meet core demands at better value for money. In particular, the RADARSAT Constellation mission is being designed for three main uses (CSA, 2013):

Table 2. *Technical details of the RADARSAT Constellation.*

Name	**RADARSAT Constellation**	
System	C-band SAR	
Operator	RSI	
Planned Launch	~ 2018	
Technical details	**Revisit time**	~ 1 day

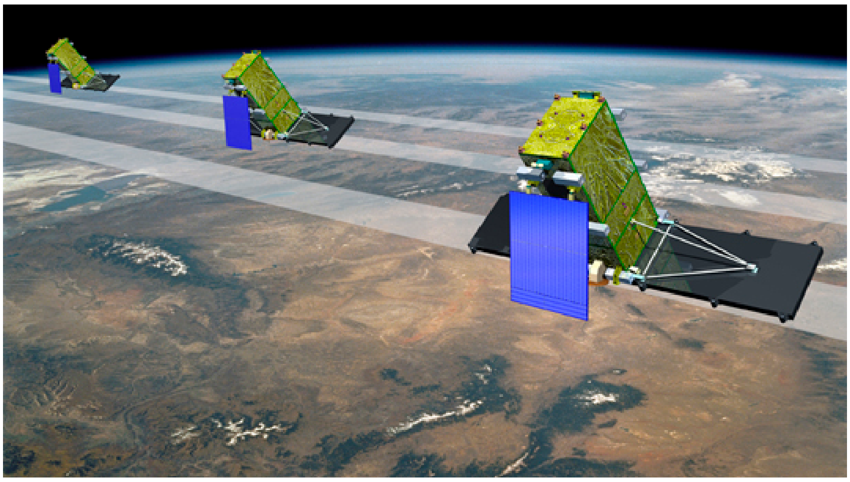

Figure 3. *Artistic impression of the RADARSAT Constellation.*

- Maritime surveillance (ice, wind, oil pollution and ship monitoring);
- Disaster management (mitigation, warning, response and recovery);
- Ecosystem monitoring (forestry, agriculture, wetlands and coastal change monitoring).

Studies demonstrating the potential of recent Radarsat data for urban applications include those of Ban & Hu (2007), Niu & Ban (2010), Li et al. (2011), or Taubenböck et al. (2012b).

2.3. TerraSAR-X2

TerraSAR-X2 is intended to insure the TerraSAR-X service continuity from 2016 onwards and to provide new VHR products with improved performance parameters to the user community. The mission will benefit from an advanced SAR sensor technology allowing a spatial resolution down to 0.25 m depending on selected and allowable chirp bandwidth. Besides the advanced Very High Resolution Modes, the TerraSAR-X2 satellite will provide heritage modes that allow direct continuity of TerraSAR-X data and improved wide swath modes to support large-area mapping. In addition, the TerraSAR-X2 mission will provide fully-polarimetric data and improved near-real-time capabilities. TerraSAR-X2 and its potential extensions will be subject to the “WorldSAR” partnership model, where partners can participate through co-investment, subscription, and up to ownership of additional

Table 3. *Technical details of TerraSAR-X2.*

Name	**TerraSAR-X2**			
System	X-band SAR			
Operator	DLR			
Planned Launch	~ 2016			
Technical details	**Acquisition mode/ Spectral resolution**	*Spotlight*	*Strip map*	*TOPS*
	Geometric resolution	0.25 m 0.5 m 1 m	3 m	5 m 12 m 30 m
	Swath	5*5 km 10*10 km 15*15 km	24 km	50 km 400 km 100 km
	Revisit time	11 days		

satellites operated in constellation. Service continuity through TerraSAR-X2 is intended to be ensured from 2016 until 2025, taking benefit of a 9.5 years satellite lifetime. The technical details of the system are presented in Table 3.

The continuation of the TerraSAR-X as well as TanDEM-X mission would allow for a systematic continuation of large-area coverage for urban monitoring. As the system perfectly fits the derivation of a new global urban layer with a significantly improved spatial resolution, this mission is predestinated to continue such efforts. Beyond the binary classification of built-up and non-built-up areas, these data even hold the potential to

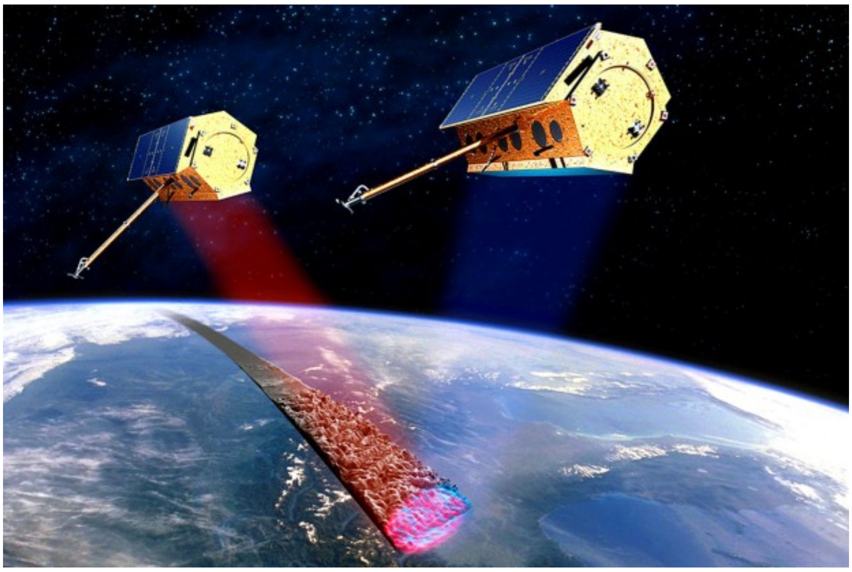

Figure 4. *Artistic impression of TerraSAR-X 2.*

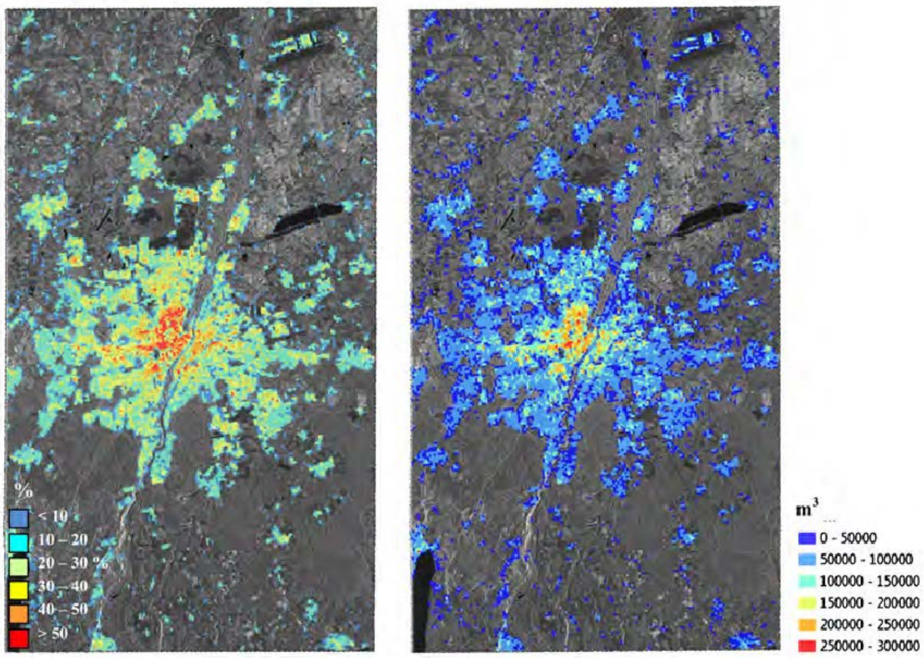

Figure 5. *Building density and building volume derived from TerraSAR-X Stripmap data (Esch et al., 2012).*

derive information on building density and building volume. An example using TerraSAR-X Stripmap data is shown in Figure 5 based on a study of Esch et al. (2012). Further applications illustrating the capabilities of data from sensors such as TerraSAR-X/TanDEM-X can be found in Ge at al. (2010) or Wang et al. (2013).

2.4. ALOS-2

The Advanced Land Observing Satellite-2 (ALOS-2) is a follow-on of the ALOS “Daichi” mission. ALOS had contributed to cartography, regional observation, disaster monitoring,

Table 4. *Technical details of ALOS-2.*

Name	**ALOS-2**			
System	L-band SAR			
Operator	JAXA			
Planned Launch	~ 2013			
Technical details	**Acquisition mode/ Spectral resolution**	*Spotlight*	*Strip map*	*Scan SAR*
	Geometric resolution	1-3 m	3-10 m	100 m
	Swath	25 km	50 or 70 km	350 or 490 km
	Revisit time	14 days		

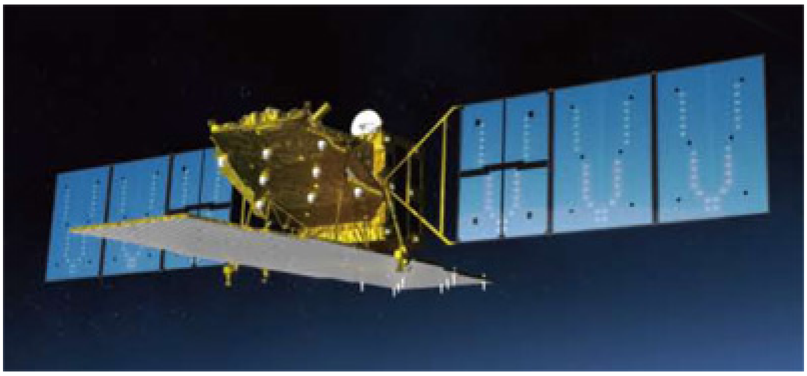

Figure 6. *Artistic impression of ALOS-2.*

and resource surveys, since its launch in 2006. ALOS-2 will succeed this mission with enhanced capabilities. Specifically, JAXA is conducting research and development activities to improve wide and HR observation technologies developed for ALOS in order to further fulfill social needs including:

1. Disaster monitoring of damaged areas, both at large scale and with high spatial detail;
2. Continuous updating of data archives related to national land and infrastructure information;
3. Effective monitoring of cultivated areas;
4. Global monitoring of tropical rain forests to identify carbon sinks.

The state-of-the-art L-band Synthetic Aperture Radar (PALSAR-2) sensor on board of ALOS-2, will operate at 1.2GHz frequency range and will offer enhanced performances compared to ALOS/PALSAR. ALOS-2 is planned to be launched by 2013 (JAXA, 2013). The technical details of the system are presented in Table 4.

The ALOS-2 mission will allow acquiring data with very large swath, hence allowing a very consistent and frequent coverage of the land surface worldwide. This will be a key aspect for fast-respond applications, as in cases of natural hazards affecting urban areas (e.g., floods, tornadoes, earthquakes). Studies demonstrating urban use cases of ALOS data are provided by Esch et al. (2008) or Ferro-Famil & Lavalle (2009).

3. Multispectral missions

3.1. Sentinel-2

The Sentinel-2 mission is scheduled to start with the launch of the first satellite in 2014. The pair of Sentinel-2 satellites will routinely deliver high-resolution optical images globally, providing enhanced continuity of SPOT- and Landsat-type data. Sentinel-2 will carry an optical payload with visible, near infrared and shortwave infrared sensors comprising 13 spectral bands: 4 bands at 10 m, 6 bands at 20 m and 3 bands at 60 m spatial resolution (the latter is dedicated to atmospheric corrections and cloud screening), with a swath width of 290 km. The 13 spectral bands guarantee consistent time series, showing variability in land surface conditions and minimizing any artifacts introduced by atmospheric variability. The mission orbits at a mean altitude of approximately 800 km and, with the pair of

Table 5. *Technical details of Sentinel-2.*

Name	**SENTINEL-2**	
System	superspectral	
Operator	ESA	
Planned Launch	~ 2014	
Technical details	**Acquisition mode/ Spectral resolution**	*Superspectral scanner with 13 bands in the visible, near infra-red and short wave infra-red*
	Geometric resolution	4 bands at 10 m, 6 bands at 20 m and 3 bands at 60 m
	Swath	290 km
	Revisit time	10 days (one satellite) / 5 days (two satellites)

satellites in operation, will have a revisit time of five days at the equator (under cloud-free conditions) and 2-3 days at mid-latitudes (ESA, 2013b). The technical details of the Sentinel-2 mission are reported in Table 5.

Continuation of the Landsat mission is of utmost relevance as this allows long-time urban monitoring. The higher spatial resolution in combination with a higher spectral resolution with a large swath enables to cover large urban areas such as mega cities at once. Thus, Sentinel-2 will provide immense potential for urban remote sensing. Improvements will allow refining the urbanized areas into structural types, such as classes based on built-up density or even to aim at classifying semantic structural types such as slum areas, central business districts or industrial sites. Thus, monitoring is not only to be continued but to be thematically way more detailed using the future Sentinel-2 mission.

Figure 8 shows the classification of an urban footprint for the entire mega city of Istanbul using the 30m resolution of Landsat. The improved technical characteristics of the

Figure 7. *Artistic impression of Sentinel-2.*

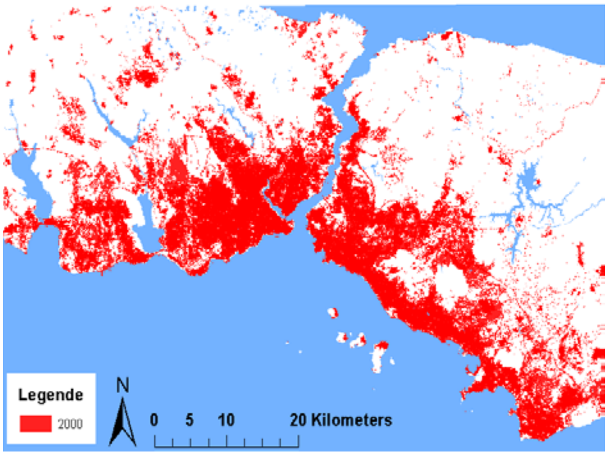

Figure 8. *Classification of the urban footprint based on Landsat TM data for the mega city of Istanbul, Turkey for the year 2000.*

Sentinel-2 mission will allow to not only continue monitoring dimension and patterns of urbanization at a relatively low thematic detail - with the classes urban, non-urban and water - but will allow to reliably achieve higher thematic details.

3.2. Sentinel-3

Sentinel-3 is a mission of the European Space Agency (ESA) to support the Global Monitoring for Environment and Security (GMES) programme. It contains to satellites, Sentinel-3A and Sentinel-3B. The first one is considered to be launched in mid-2014 whereas the launch of the second one is planned to take place 12 to 18 months later. As a part of the Sentinel satellites for earth observation, the task of Sentinel-3 is the detection of the topography of the sea surface. Therefore the two satellites have a certain amount of payload such as an Ocean and Land Colour Instrument (OLCI), a Sea and Land Surface Temperature Radiometer (SLSTR), the Sentinel-3 Ku/C Radar Altimeter (SRAL), a Microwave Radiometer (MWR) and a Precise Orbit Determination (POD). OLCI and SLSTR acquire in 21 and 9 bands, respectively (EO-Portal, 2013a).

Table 6. *Technical details of Sentinel-3.*

Name	**SENTINEL-3**	
System	multispectral	
Operator	ESA	
Planned Launch	~ 2014	
Technical details	**Acquisition mode/ Spectral resolution**	*Multispectral scanner with 30 bands in the visible, near infra-red, thermal infra-red and short wave infra-red*
	Geometric resolution	1200 m, 300 m, 1000 m, 500 m
	Swath	1270 m, 750 m, 1800 m
	Revisit time	27 days

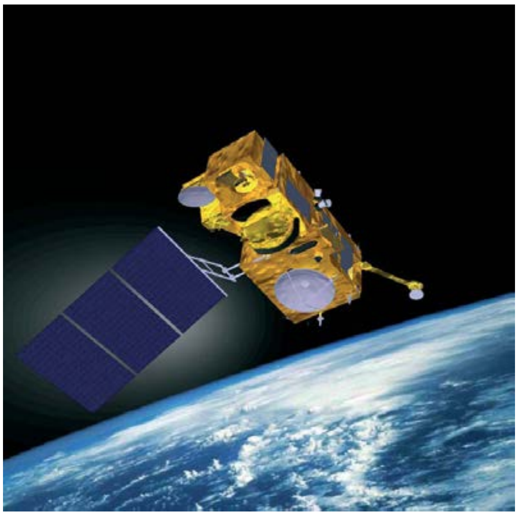

Figure 9. *Artistic impression of Sentinel-3.*

Due to those different instruments, there are various resolutions and swaths. The swath of OLCI is 1270 km, the one of SLSTR is between 740 km and 1400 km, depending of nadir or oblique measuring, SRAL has a footprint of > 2 km and the MWR one is 20 km. Sentinel-3 will be located in an altitude of 815 km and according to its polar orbit it will cover the whole earth every 27 days. OLCI has a spatial resolution of 300 m whereas the spatial resolution of SLSTR depends of the bands and is between 500 m and 1 km. In terms of the accuracy the other instruments have values of 3 cm for SRAL and POD whereas the accuracy of MWR is 3 K (ESA, 2012c). Table 6 shows the technical details of the Sentinel-3 mission.

The main task of Sentinel-3 is the observation of the sea surface topography. The satellites can provide data concerning parameters such as the sea surface colour, the sea surface temperature or the altitude of waves. The data, the satellite provides, is not only used for sea surface analysis but also for monitoring of other environmental issues which don't contain the sea surface. Due to its high accuracy, the output data can be used in many different ways and for a variety of research tasks (ESA, 2012c). Figure 9 shows an artistic impression of the Sentinel-3 satellite.

3.3. Landsat 8

The Landsat 8 mission is part of the Landsat Data Continuity Mission (LDCM) on behalf of the NASA and the US Geological Survey (USGS). The mission was launched on February

Table 7. *Technical details of Landsat 8.*

Name	**Landsat 8**	
System	multispectral	
Operator	NASA / USGS	
Planned Launch	February 11, 2013	
Technical details	**Acquisition mode/ Spectral resolution**	*Multispectral and panchromatic scanner with nine bands in the visible, near infra-red, short wave infra-red and panchromatic*
	Geometric resolution	15 m panchromatic 30 m multi-spectral
	Swath	185 km
	Revisit time	16 days

11, 2013. The new satellite provides in parts the same technique as the former Landsat satellites. Nevertheless there are some changes which allow a better data. The payload of Landsat 8 consists of an Operated Land Imager (OLI) and a Thermal Infrared Sensor (TIRS). Including the TIRS with two spectral bands, the whole Landsat 8 is able to measure with nine bands. The techniques of these bands are mostly the same as in the payload of Landsat 8's predecessors. The only differences in the OLI sensor are a blue band for coastal measures and a shortwave-infrared band which is able to detect clouds. Those bands provide over 7000 detections per spectral band. The Landsat 8 is located in the near-polar orbit in an altitude of 705 m. It gets a full image of the earth every 16 days.
The spatial resolution of OLI is 15 m for panchromatic and 30 m for multi-spectral while the swath is 185 km. Using the same swath, the TIRS spatial resolution is 100 m. The important newness of the TIRS is the use of quantum mechanics. So-called Quantum Well Infrared Photodetectors (QWIPs) work with two spectral bands to get a more exact value for the earth's temperature. Depending on this technique it is possible to separate the land surface temperature from the atmospheric temperature. Another advantage of QWIPs are the low costs (NASA, 2013b). Table 7 shows the technical details of the Landsat 8 mission.
The main task for Landsat 8 is to provide data of the land surface. It is possible to detect the land use of an area such as farms, forests or cities. This is possible for continental land as well as coastal lines, islands and the Polar Regions. The TIRS is able to measure different temperatures of water. Therefore this satellite is mainly important for showing the

Figure 10. *Artistic impression of Landsat 8.*

water use. Nevertheless the land use and the changing of the environment are also observed by this mission. In general the Landsat missions have the aim to detect changes of the land surface and the land use. Therefore a comparison of the different Landsat satellites is made (NASA, 2013b). The artistic impression of Landsat 8 is shown on Figure 10.

3.4. ALOS-3

ALOS-3 is the follow-on of the ALOS/Daichi optical mission and will complement the SAR services of the ALOS-2 mission.

ALOS-3 will mount an optical sensor complement to succeed PRISM (Panchromatic Remote-sensing Instrument for Stereo Mapping) and AVNIR-2 (Advanced Visible and Near-Infrared Radiometer-2) on board of ALOS. The goal of the ALOS-3 mission is to provide operational support services in the following areas:

1) Disaster monitoring of stricken regions;
2) Continuous updating of data archives related to national geographical information (including topographic maps, land use, and vegetation);
3) Survey of crops and coastal fishing conditions;
4) Environmental monitoring, including illegal dumping of industrial wastes.

The basic requirements include high resolution, wide swath, prompt observation and information delivery after a disaster (EO-Portal, 2013b). The technical details of the mission are presented in Table 6.

Table 8. *Technical details of ALOS-3.*

<table>
<tr><th>Name</th><th colspan="2">ALOS-3</th></tr>
<tr><td>System</td><td colspan="2">multispectral</td></tr>
<tr><td>Operator</td><td colspan="2">JAXA</td></tr>
<tr><td>Planned Launch</td><td colspan="2">~ 2015</td></tr>
<tr><td rowspan="4">Technical details</td><td>Acquisition mode/
Spectral resolution</td><td>Multispectral scanner with high stereo acquisition capability</td></tr>
<tr><td>Geometric resolution</td><td>0.8 m</td></tr>
<tr><td>Swath</td><td>50 km</td></tr>
<tr><td>Revisit time</td><td>14 days</td></tr>
</table>

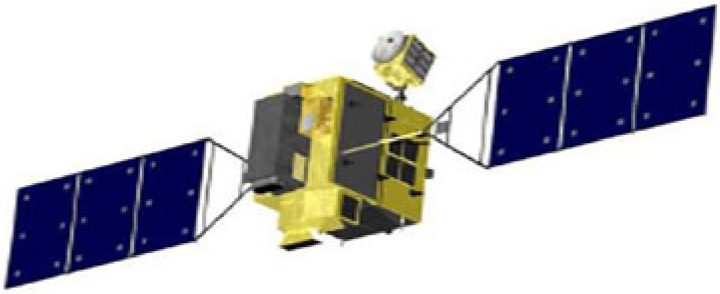

Figure 11. *Artistic impression of ALOS-3.*

It is worth noting that the capability of providing HR data with 50 km swath will allow area-wide city classification (i.e., a 50 km swath indeed often covers entire metropolitan areas). The classification illustrated in Figure 12 is based on an object-oriented approach (Taubenböck et al., 2010a) that has been applied to data from the IKONOS sensor, which exhibits features very close to those of the upcoming ALOS-3 mission.

However, the IKONOS sensor only has a swath width of 11 km. Thus, it becomes obvious which capabilities the ALOS-3 sensor for urban classifications and applications will offer. In this context, several analyses on urban structure types (e.g., Wurm et al., 2009), energy-relevant questions (e.g., Geiß et al., 2011), as well as on risk and vulnerability (e.g., Taubenböck et al., 2009) have been carried out in the literature.

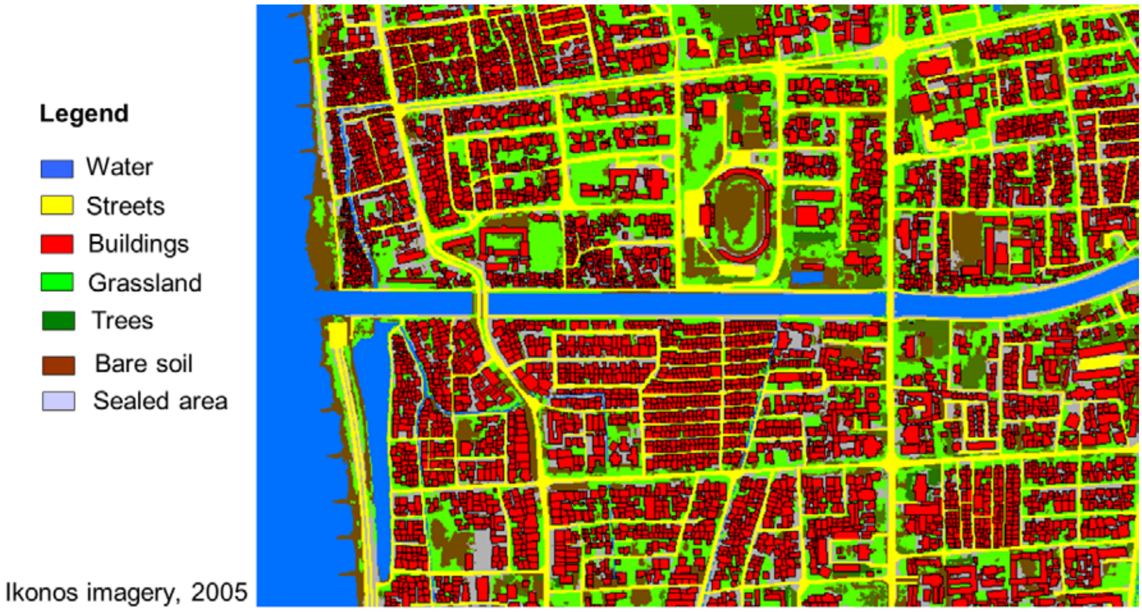

Figure 12. *Result of object-based classification of an urban environment using IKONOS data, comparable to the future ALOS-3 image properties.*

Table 9. *Technical details of Cartosat-3.*

Name	**Cartosat-3**	
System	panchromatic	
Operator	ISRO	
Planned Launch	~2014	
Technical details	**Acquisition mode/ Spectral resolution**	*Panchromatic scanner*
	Geometric resolution	0.25 m
	Swath	6 km

3.5. Cartosat-3

The Indian Space Research Organization (ISRO) plans to launch the new VHR Cartosat-3 satellite in 2014, which will be capable of acquiring images at 0.25 m spatial resolution. This will represents the finest resolution ever supported by any commercial spaceborne satellite (nowadays the record belongs to GeoEye-1 which was launched in 2008 and allows to acquire panchromatic images at 0.41 m spatial resolution). Besides urban applications, key potential uses include weather mapping, cartography, and strategic applications. Beyond this, stereo mapping is of high importance for urban applications as cities do not only feature a 2-dimensional layout but also a 3-dimensional. From the combination of optical VHR data and a digital surface model, a 3-dimensional city model

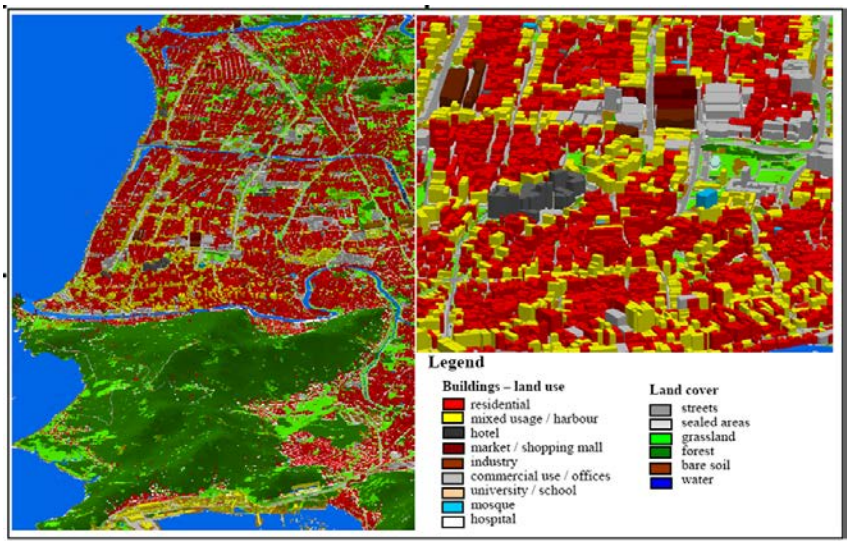

Figure 13. *3D city model of the city of Padang (Indonesia) derived from the combined analysis of IKONOS imagery and SRTM DEM (from Taubenböck et al. 2009).*

Table 10. *Technical details of WorldView-3.*

Name	**WorldView-3**	
System	multispectral	
Operator	Digital Globe	
Planned Launch	~2014	
Technical details	**Acquisition mode/ Spectral resolution**	*Multispectral scanner with 29 bands in the visible, near infra-red, thermal infra-red, short wave infra-red, panchromatic and CAVIS*
	Geometric resolution	1 band at 0.31 m, 8 bands at 1.24 m, 8 bands at 3.7 m, 12 bands at 30 m
	Swath	At nadir 13.1 km
	Revisit time	< 1 day

can be generated that allows the analysis of urban morphologies in high spatial detail. Figure 13 provides a 3D perspective view (derived from IKONOS imagery and SRTM DEM) on the city of Padang Indonesia and gives a glimpse of the vertical structures, the densities, the pattern and alignment of open spaces, building types, etc.

3.6. WorldView-3

With respect to current VHR sensors as WorldView-2 or Cartosat-1 (which allow the derivation of digital surface models from stereo imaging), WorldView-3 (DigitalGlobe, 2013), will be the first multi-payload, superspectral, VHR commercial satellite. Operating at an expected altitude of 617 km, WorldView-3 will be launched in 2014 and provide imagery at 0.31 m spatial resolution in the panchromatic channel, 1.24 m spatial resolution in the visible portion of the spectrum, and 3.7 m spatial resolution in the short-wave infrared. WorldView-3 has an average revisit time of <1 day (however with different imaging angles) and is capable of imaging up to 680,000 km^2 per day, further enhancing the possibilities of near-real-time data collection.

Moreover, this will also boost the development of VHR digital surface models, which are of paramount importance for characterizing urban morphology. Indeed, so far 3-D city models derived from EO data are often limited to small areas (due to the limited acquisition capability of current sensors) not properly covering entire metropolitan areas.

It is worth noting that availability of stereo data in the next future will be then guaranteed by several upcoming missions; nevertheless, data cost is still expected to be a bottleneck for their operational employment.

Figure 14. *Artistic impression of WorldView-3.*

4. Hyperspectral missions

Several spaceborne hyperspectral missions are currently in a planning and development stage and in few years they will provide data on regular operational basis. These initiatives include the HISUI mission (Hyperspectral Imager SUIte) (Kawashima et al., 2010), the HyspIRI mission (Hyperspectral Infrared Imager) (Green et al., 2008) and the EnMAP mission (Environmental Mapping and Analysis Program) (Kaufmann et al., 2006).

4.1. EnMAP

The German EnMAP (Environmental Mapping and Analysis Programme) mission will mount a novel space borne imaging spectrometer with 30 m spatial resolution and a high signal-to-noise ratio, namely the Hyperspectral Imager (HSI). Figure 15 shows an artist's view of the satellite. The HSI sensor will observe the sunlight reflected from Earth across a wide range of wavelengths ranging from the visible to the short wave infrared.

This will make it possible to accurately study the condition of the Earth's surface and the changes affecting it. The mission is scheduled to be launched in 2017 and is designed to continuously operate for five years. The expected high data quality and its extensive spatial coverage of 900 km^2 per scene will open up possibilities for the upscaling of existing imaging spectroscopy approaches developed for airborne data with limited spatial coverage. However, a direct transfer of these methods to spaceborne imaging spectroscopy data will be challenging because of the difference in spatial resolution between the airborne and EnMAP HSI data. EnMAP is expected to definitely support finding global answers to a range of questions dedicated to environmental, agricultural, land use, water management and geological issues. In this context, new or adapted methods will be required to effectively exploit the full information content of the EnMAP HSI data for urban analysis (Heldens et al., 2011) in order to properly characterize thematic details of different settlements.

Heldens et al. (2011) reviewed 146 publications to give an outlook on the capabilities of the EnMAP mission. In particular, four main application fields regarding the urban topic have been identified:

Table 12. *Technical details of EnMAP.*

Name		**EnMAP**
System		hyperspectral
Operator		DLR / GFZ
Planned Launch		~ 2017
Technical details	**Acquisition mode/ Spectral resolution**	*Hyperspectral scanner at 6 VNIR and 10 SWIR with a spectral range between 420 and 2450 nm*
	Geometric resolution	30 m
	Swath	At nadir 30 km
	Revisit time	4 days

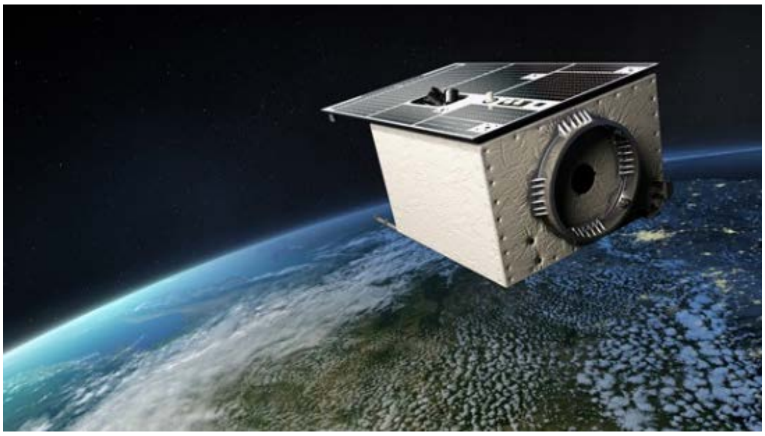

Figure 15. *Artistic impression of EnMAP.*

1) urban development and planning;
2) urban growth assessment;
3) risk and vulnerability assessment;
4) urban climate.

Concerning urban development and planning EnMAP can improve the local to regional mapping of built-up areas, imperviousness, vegetation fraction, surface materials, urban structure types and biotopes. Regarding urban growth assessment, fine spectral resolution and high spatial resolution will allow to improve the delineation of urban extent (in particular it will ease the differentiation between built up areas and bare soil and bare rock) and hence reliably identify changes in time. In the context of risk and vulnerability assessment, hazardous materials detection is expected to be significantly improved and in the framework of urban climate applications improved mapping capabilities of material-based land cover as well as buildings and vegetation structures will be an asset. Table 12 shows the technical details of EnMAP.

4.2. HyspIRI

The design of the Hyperspectral Infrared Imager (HyspIRI) mission is focus on studying the world’s ecosystems and provide critical information on natural disasters such as volcanoes, wildfires and droughts.

The mission is expected to be launched by 2020 (CEOS 2013). With a spatial resolution of 60 m this sensor is not expected to exhibit the same performances of EnMAP to characterize the urban environment. However, with a 600 km swath width the HyspIRI mission will allow large area monitoring of urban areas at continental or global scale. Artistic impression of the satellite is reported in Figure 16, whereas technical details are shown in Table 13.

Table 13. *Technical details of HyspIRI.*

Name	**HyspIRI**		
System	hyperspectral		
Operator	NASA		
Planned Launch	~ 2020		
Technical details	**Acquisition mode/ Spectral resolution**	*Hyperspectral 10 VNIR Spectral range 400-2500 nm*	*TIR 80 SWIR Spectral range 4000-12000 nm*
	Geometric resolution	60 m	60 m
	Swath	At nadir: 145 km	At nadir: 145 km
	Revisit time	19 days	

4.3. HISUI

HISUI is the short name for Hyperspectral Image Suite Project on behalf of the Japanese Ministry of Economy, Trade and Industry (NASA, 2012). After OPS, ASTER and ASNARO, HISUI is the 4th optical image instrument which is planned to be launched at the earliest in 2015. It will be on board of the ALOS-3 satellite. HISUI contains on the one hand a multispectral and on the other hand a hyperspectral imager. The multispectral imager has a spatial resolution of 5 m with a swath of 90 km. The spatial resolution of the hyperspectral imager is 30 m with a swath of 30 km. While the multispectral sensor has only 4 bands, the hyperspectral one consists of 185.

The mission of HISUI will be inter alia the area mapping, engineering observation or emergency and disaster observation. Furthermore the instrument will be launched to do observe the environmental changes. In particular the monitoring of gas, oil and metal

Table14. *Technical details of HISUI.*

Name	**HISUI**		
System	hyperspectral		
Operator	Japanese Ministry of Economy, Trade and Industry		
Planned Launch	~ 2015		
Technical details	**Acquisition mode/ Spectral resolution**	*Hyperspectral 10 VNIR / 12,5 SWIR Spectral range 400-2500nm*	*Multispectral TBA Spectral range 450-900nm*
	Geometric resolution	30m	5m
	Swath	30km	90km
	Revisit time		

resources plays an important role for the observation task. Table 14 shows the technical details of HISUI.

4.4. Summary of technical details of future missions

Table 15 shows, as a summary, the technical details of all mentioned missions in the essay at hand. It is divided into the three system categories and displays technical parameters as the spectral and geometric resolution, the swath and the launch date. The detailed listing of every parameter related to the others allows a survey of the technical details in a single look. The spectral range is reported in the second column, whereas the

Figure 16. *Artistic impression of HyspIRI.*

third and fourth columns describe the geometric resolution and the swath, respectively.

The launch date in the last column provides additional information about the progressing of the missions.

Table 15. *Summary of technical details for all the considered missions.*

	Mission	Spectral resolution	Geometric resolution	Swath	Launch date
Radar	**Sentinel-1**	C-band SAR	5*20 m / 5*5 m	250 km / 20 km	~ 2013
	RADARSAT Constellation	C-band SAR			~ 2018
	TerraSAR-X2	X-band SAR	0.25 m / 3 m / 5 m 0.5 m / 3 m / 12 m 1 m / 3 m / 30 m	5*5 km / 24km / 50 km 10*10 km / 24km / 400 km 15*15 km / 24km / 100 km	~ 2016
	ALOS-2	L-band SAR	1-3 m / 3-10 m / 100 m	25 km / 50 or 70 km / 350 or 490 km	~ 2013
Multispectral	**Sentinel-2**	4 bands (VNIR, Blue, Green, Red)	10 m	290 km	~ 2014
		6 bands (VNIR, SWIR)	20 m		
		3 bands (VNIR, SWIR)	60 m		
	Sentinel-3	OLCI: 21 bands (VIS)	1200 m (ocean) 300 m (coastal, land)	1270 km	~ 2014
		SLSTR and AATSR: 9 bands (VIS, SWIR, MWIR-TIR)	500 m	Dual view swath 750 km	
			1000 m	Nadir swath 1800 km	
	Landsat 8	8 bands (New Deep Blue, Blue, Green, Red, NIR, SWIR 2, SWIR 3, SWIR)	30 m	185 km	February 11, 2013
		1 band (PAN)	15 m		
	ALOS-3	4 bands (0.42-0.89µm) 1 band (PAN)	0.8 m	50 km	~ 2013
	Cartosat-3	1 band (PAN)	0.25 m	6 km	~ 2014
	WorldView-3	1 band (PAN)	0.31 m	At nadir 13.1 km	~ 2014
		8 bands (Blue, Green, Red, near-IR1, coastal, yellow, red edge, near IR-2)	1.24 m		
		8 bands (SWIR)	3.7 m		
		12 bands (CAVIS)	30 m		
Hyperspectral	**EnMAP**	Hyperspectral 6 VNIR / 10SWIR Spectral range: 420-2450 nm	30 m	At nadir 30km	~ 2017
	HyspIRI	Hyperspectral / TIR	Hyperspectral / TIR	Hyperspectral / TIR	~ 2020
		10 VNIR / 80 SWIR / 400 TIR Spectral range: 400-2500 nm / Spectral range: 4000-12000 nm	60 m / 60 m	At nadir 145 km / At nadir 600 km	
	HISUI	Hyperspectral / Multispectral	Hyperspectral / Multi-spectral	Hyperspectral / Multi-spectral	~ 2015

5. Contribution of future missions to current and novel indicators

Both, the recently launched as well as the future satellite missions described in the previous chapters hold certain potential to foster and improve the derivation of parameters and indicators on the urban environment. The new SAR and multispectral systems mainly guarantee a continued provision of the hitherto existing EO data sets and analysis procedures. Therewith, the linked applications and calculation of basic parameters and indicators such as the ones demonstrated in the GEOURBAN project can be carried forward - a central prerequisite for monitoring tasks based on mid- and long-term time series data sets. At the same time it is expected that the framework conditions and quality of EO-based analyses can be increased since central properties of the new sensors - such as the temporal and spatial coverage, the geometric and in some case also the spectral and radiometric resolution - have been or will be improved considerably. However, these improvements also come along with an increased product size and amount of data. This leads to rising demands on the processing capabilities and efficiency of the analysis methods and techniques. This is in particular true with respect to the availability of mass data sets such as those expected to be provided by the Sentinel-2 mission. Accordingly, in the near future the derivation of urban indicators will rather be an issue of efficient data processing and effective choice of the optimal sensor system and constellation rather than getting access to suitable EO data (which had been so far the main limitation in urban remote sensing).

In contrary to the future SAR and multispectral missions, the upcoming hyperspectral missions such as EnMAP, HyspIRI or HISU provide completely new opportunities that will also come along with the demand for developing adapted image analysis techniques and applications. Hence, the main focus of this chapter is now set on the expected challenges and contributions of these future spaceborne hyperspectral missions.

In general, airborne imaging spectroscopy has been invented in the nineties and has mainly been focused on the thematically detailed mapping of urban surface materials.

Thereby, a high potential was identified with respect to the combination of airborne hyperspectral imagery and laboratory and field measurements (Ben-Dor et al., 2001; Heiden et al., 2007; Herold et al., 2004). However, the benefits of spaceborne imaging spectrometers for urban studies have not yet been fully analyzed and explored. One of the main reasons is the so far limited availability of spaceborne imaging spectroscopy data such as collected by NASA's Hyperion sensor (Ungar et al., 2003) or ESA's CHRIS-PROBA (Cutter et al., 2004) instrument, as shown by the studies of Weng et al. (2008), Xu & Gong (2007) or Cavalli et al. (2008).

Moreover, spaceborne imaging spectrometers show a significantly lower spatial resolution than the actual multispectral systems. This is in particular critical since the typical small-scale urban objects, such as buildings or streets, cannot be resolved properly. However, based on a literature review, Heldens et al. (2011) demonstrate that a wide range of urban EO applications - i.e., the monitoring of the development of built-up areas, imperviousness or vegetation -, is still based on the analysis of HR multispectral data. Therefore the new hyperspectral satellite systems will improve the quality and accuracy of urban indicators at least with respect to analyses at regional scale where HR data are most applicable. This characteristic is mainly due to the enhanced ability of hyperspectral sensors to provide a material-based inventory of the urban environment. For instance, with current spaceborne multispectral sensors the mapping of a key parameter such as the percent impervious surface is often limited due to the difficulty of separating impervious surfaces (e.g., asphalt, concrete) from bare soil. Using spaceborne hyperspectral imagery the within-class variation of impervious surfaces as well as that of soil can be taken into account, thus improving the accuracy of imperviousness estimations (Weng et al., 2008). Studies by Xu & Gong (2007) and Cavalli et al. (2008) also show that the immense spectral resolution of hyperspectral systems is their most significant strength compared to multispectral sensors since this capability allows for a material-based identification of urban land cover types.

The above-mentioned studies show that the discrimination of the various land cover types is a central component in most urban applications. Therefore, the development of improved and adapted methods for a material-oriented urban land cover mapping will be a key issue in future when focusing on the derivation of urban indicators and parameters.

Nevertheless, in this context improved sub-pixel analyses and spectral unmixing approaches will become vital to cope with the limited size and the high heterogeneity of the man-made objects forming the urban landscape (Cavalli et al., 2008; Small, 2001; Powell et al., 2007). Thereby, the definition of pure pixels for training or the definition of endmember data sets will still be challenging due to the restricted geometric resolution. A promising solution might be provided by the integration of external spectral image libraries measured as prior knowledge for sub-pixel analyses. However, considering the global acquisition capabilities of spaceborne hyperspectral sensor systems, specific libraries are certainly not applicable to all areas of interest and thus have to be collected individually - at least for the main urban ecoregions as introduced by Schneider et al. (2010). Taking into account the spectral resolution of spaceborne hyperspectral imagery we assume that it is worth investigating the utilization of predefined mixed spectra within those spectral libraries. Although these mixed spectra will differ regionally and globally (Bochow et al., 2010), their use is supposed to be a promising alternative to the integration of pure material spectra.

Spectral libraries can also be used for classification purposes by comparing the image pixel spectra with a library spectrum. This has been realized for example with the Tetracorder system (Clark et al., 2003) and could also be an option for identifying typical urban surface material mixtures. Such an approach requires the recognition of mixed spectra by specific spectral reflectance characteristics such as absorption features. Another promising approach applying spectral comparison measures such as presented by Chang (2000) is introduced by Mende et al. (2011), who evaluate the significance of spectral comparison values according to the mixture information.

We can also expect that the derivation of indicators describing trends of urbanization (multi-temporal change analysis) will profit from the emergence of spaceborne hyperspectral systems (Taubenböck et al., 2010b; Scheider et al. 2010). Indeed, the analysis of time series data for the quantitative and qualitative characterization of the spatiotemporal development of urban agglomerations helps to gain more precise knowledge on the status and dynamics of urban systems. However, a certain challenge with respect to indicators and parameters describing multi-temporal properties derived from hyperspectral satellite data is the occurrence of BRDF (bidirectional reflectance distribution function) effects. Time series images will be collected with differing viewing conditions and this will affect the spectral signatures of the pixels. Accordingly, the BRDF of the various urban surfaces has to be taken into account in the context of an analysis of hyperspectral satellite imagery. The BRDF of urban surfaces has been investigated by Meister et al. (1998) and a large-scale bidirectional reflectance model for urban areas was developed by Meister et al. (2001) for imaging systems with a spatial resolution of more than 500 x 500 m. However, in consideration of the improved spatial resolution of the new systems these models have to be adjusted and further improved.

A certain number of the indicators addressed in the context of the GEOURBAN project aims at the characterization of urban land cover and structures at the local scale. Although the new HR hyperspectral satellite sensors will not allow for the direct mapping of the small-scale urban objects, image data fusion techniques will provide valuable possibilities for analyses at local scale (Zhang, 2010). As an example, concerning EnMAP, the iconic data fusion at pixel or signal level is particularly interesting and various methods have been developed on iconic image fusion, where panchromatic images with high spatial resolution are combined with multispectral images of low spatial but higher spectral resolution (Ehlers et al., 2010). A key issue in that context is to avoid spectral distortions when increasing the spatial resolution. Hence, spectrum-preserving fusion techniques - such as presented by Ehlers et al. (2004), Ehlers (2007) or Palubinskas & Reinartz (2011) - will become particularly important. At the same time, data fusion holds certain potential to foster the use of indicators describing the urban climate since the fusion techniques allow for the extension of the hyperspectral data, e.g., by thermal information provided by other sensors (Xu et al., 2008).

In conclusion, one can state that the upcoming spaceborne hyperspectral missions will improve the capabilities to derive parameters and indicators on the urban environment. Although there is a discrepancy between the average size of urban objects and the spatial resolution of the future hyperspectral satellite sensors, there is still potential to benefit from the more capacious and precise spectral information content of the corresponding imagery. However, in view of the comparably low spatial resolution there is still a need for research into improved spectral unmixing methods providing information on the proportion of the different urban surface or material types within a pixel. An important step in this context is the generation and use of simulated hyperspectral satellite data sets for urban areas. Guanter et al. (2009) present a tool that allows generating simulated EnMAP data for several natural environments, acquisition and illumination geometries, cloud cover situations, and instrument configurations. For the simulation of an urban scene, additional BRDF effects have to be taken into account by using a high resolution surface model (DSM) of the built-up area. This enables the retrieval of surface reflectance by considering the complex radiative transfer processes due to the urban structure (Richter & Müller, 2005; Lacherade et al., 2008) and thus, helps to better understand the spectral mixture characteristics of an urban scene.

6. References

Ban, Y.; Hu, H. (2007): RADARSAT fine-beam SAR data for land-cover mapping and change detection in the rural-urban fringe of the Greater Toronto Area. In 2007 Urban Remote Sensing Joint Event, URS, 11-13 April 2007, Paris, France.

Ben-Dor, E.; Levin, N.; Saaroni, H. (2001): A spectral based recognition of the urban environment using the visible and near-infrared spectral region. A case study over Tel-Aviv, Israel. International Journal of Remote Sensing, vol. 22, pp. 2193-2218.

Bochow, M.; Taubenböck, H.; Segl, K.; Kaufmann, H. (2010): An automated and adaptable approach for characterizing and partitioning cities into urban structure types. Proceedings of IGARSS 2010, 25-30 July 2010, Honolulu, Hawaii, USA, pp. 1796-1799.

Cavalli, R.M.; Fusilli, L.; Pascucci, S.; Pignatti, S.; Santini, F. (2008): Hyperspectral Sensor Data Capability for Retrieving Complex Urban Land Cover in Comparison with Multispectral Data: Venice City Case Study (Italy). Sensors, vol. 8, pp. 3299-3320.

CEOS (2013): http://database.eohandbook.com/database/missionsummary.aspx?missionID=644, 20/07/13.

Chang, C. (2000): An information theoretic-based approach to spectral variability, similarity and discriminability for hyperspectral image analysis. IEEE Transactions on Information Theory, vol. 46, pp. 1927-1932.

Clark, R.N.; Swayze, G.A.; Livo, K.E.; Kokaly, R.F.; Sutley, S.J.; Dalton, J.B.; McDougal, R.R.; Gent, C.A. (2003): Imaging spectroscopy: Earth and planetary remote sensing with the USGS Tetracorder and expert systems. Journal of Geophysical Research-Planets, vol. 108, pp. 5131.

CNES (2013): http://www.cnes.fr/web/CNES-en/1415-spot.php, 20/07/13.

CSA (2013): http://www.asc-csa.gc.ca/eng/satellites/default-eo.asp, 20/07/13.

Cutter, M.A.; Johns, L.S.; Lobb, D.R.; Williams, T.L.; Settle, J.J. (2004): Flight experience of the Compact High Resolution Imaging Spectrometer (CHRIS). Proceedings of SPIE - The International Society for Optical Engineering, vol. 5159, no. 1, pp. 392-405.

DigitalGlobe (2013): http://www.digitalglobe.com/about-us/content-collection, 20/07/13.

DLR (2013a): http://www.dlr.de/eo/en/desktopdefault.aspx/tabid-5725/9296_read-15979/, 20/07/13.

DLR (2013b):http://www.dlr.de/hr/en/desktopdefault.aspx/tabid-2317/, 20/07/13.

Ehlers, M.; Klonus, S. (2004): Erhalt der spektralen Charakteristika bei der Bildfusion durch FFT basierte Filterung. Photogrammetrie - Fernerkundung - Geoinformation, vol. 6, pp. 495-506.

Ehlers, M. (2007): Segment based image analysis and image fusion. ASPRS 2007 Annual Conference Tampa, Florida.

Ehlers, M.; Klonus, S.; Johan, R.P.; Rosso, P. (2010): Multi-sensor image fusion for pansharpening in remote sensing. International Journal of Image and Data Fusion, vol. 1, pp. 25-45.

EO-Portal (2013a): https://directory.eoportal.org/web/eoportal/satellite-missions/c-missions/copernicus-sentinel-3#foot24%29, 20/07/13.

EO-Portal (2013b): https://directory.eoportal.org/web/eoportal/satellite-missions/a/alos-3, 20/07/13.

EnMAP (2013): http://www.enmap.org/, 20/07/13.

ESA (2013a): https://earth.esa.int/web/guest/missions/esa-operational-eo-missions/envisat/instruments/meris, 20/07/13.

ESA (2013b): http://www.esa.int/Our_Activities/Operations/GMES_Sentinels, 20/07/13.

ESA (2012c): http://esamultimedia.esa.int/docs/S3-Data_Sheet.pdf, 20/07/13

Esch, T.; Roth, A.; Thiel, M.; Schmidt, M.; Dech, S. (2008): Comparison of ALOS-PALSAR and TerraSAR-X data in terms of detecting settlements - first results. Proceedings of ALOS PI Symposium 2008, 3-7 November 2008, Rhodes, Greece.

Esch, T., Thiel, M., Schenk, A., Roth, A., Mehl, H., & Dech, S. (2010). Delineation of urban footprints from TerraSAR-X data by analyzing speckle characteristics and intensity information. IEEE Transactions on Geoscience and Remote Sensing. vol. 48, no. 2, pp. 905-916.

Esch, T.; Taubenböck, H.; Roth, A.; Heldens, W.; Felbier, A.; Thiel, M.; Schmidt, M.; Müller A.; Dech, S. (2012): TanDEM-X mission: New perspectives for the inventory and monitoring of global settlement patterns. In: Journal of Selected Topics in Applied Earth Observation and Remote Sensing, vol. 6, p.22.

Ferro-Famil, L.; Lavalle, M. (2009): Detection and Analysis of Urban Areas using ALOS PALSAR Polarimetric Data. Proceedings of IGARSS 2009, 12-17 July 2009, Cape Town, South Africa, pp. 142-145.

Gamba, P.; Lisini, G. (2012): A robust approach to global urban area extent extraction using ASAR Wide Swath Mode data," Proc. of Tyrrhenian Workshop 2012 on Advances in Radar and Remote Sensing (TyWRRS), 12-14 September 2012, Naples, Italy, pp. 1-5.

Ge, D.; Yan, W.; Zhang, L.; Guo, X.; Xia, Y. (2010): Mapping urban subsidence with TerraSAR-X data by PSI analysis. Geoscience and Remote Sensing Symposium (IGARSS) 2010, 25-30 July 2010,

Green, R.; Asner, G.; Ungar, S.; Knox, R (2008): NASA Mission to Measure Global Plant Physiology and Functional Types. Proceedings of 2008 IEEE Aerospace Conference, 1-8 March 2008, Big Sky, MT, USA.

Guanter, L.; Segl, K.; Kaufmann, H. (2009): Simuation of the optical remote-sensing scences with application to the EnMAP hyperspectral mission. IEEE Transactions on Geoscience and Remote Sensing, vol. 47, pp. 2340-2351.

Hay, G.; Blaschke, T. (2011): "Urban Remote Sensing", Special Issue in Remote Sensing http://www.mdpi.com/journal/remotesensing/special_issues/urban_rs, 20/07/13.

Heiden, U.; Segl, K.; Roessner, S.; Kaufmann, H. (2007): Determination of robust spectral features for identification of urban surface materials in hyperspectral remote sensing data. Remote Sensing of Environment, vol. 111, pp. 537-552.

Heldens, W., Heiden, U., Esch, T., Stein, E.; Müller, A. (2011): Can the Future EnMAP Mission Contribute to Urban Applications? A Literature Survey. Remote Sensing, vol. 3, no. 9, pp. 1817-1846.

Herold, M.; Roberts, D.A.; Gardner, M.E.; Dennison, P.E. (2004): Spectrometry for urban area remote sensing - Development and analysis of a spectral library from 350 to 2400 nm. Remote Sensing of Environment, vol. 91, pp. 304-319.

ISRO (2013): http://www.isro.org/satellites/earthobservationsatellites.aspx, 20/07/13.

JAXA (2013): http://www.eorc.jaxa.jp/ALOS/en/about/about_index.htm, 20/07/13.

Jiang, L.-M.; Liao, M.-S.; Lin, H. (2008): Estimating urban impervious surface percentage with ERS-1/2 InSAR data. J. Remote Sens. Beijing, vol. 12, no. 1, pp. 184-191.

Kaufmann, H.; Segl, K.; Chabrillat, S.; Hofer, S.; Stuffler, T.; Müller, A.; Richter, R.; Schreier, G.; Haydn, R.; Bach, H. (2006): A Hyperspectral Sensor for Environmental Mapping and Analysis. Proceedings of IGARSS 2006 & 27th Canadian Symposium on Remote Sensing, 31 July-4 August 2006, Denver, CO, USA.

Kawashima, T.; Narimatsu, Y.; Inada, H.; Ishida, J.; Hamada, K.; Ito, Y.; Yoshida, J.; Ohgi, N.; Tatsumi, K.; Harada, H.; Kawanishi, T.; Sakuma, F.; Iwasaki, A. (2010): The functional evaluation model for the on-board hyperspectral radiometer. Proceedings of SPIE 7857, Multispectral, Hyperspectral, and Ultraspectral Remote Sensing Technology, Techniques, and Applications III.

Lacherade, S.; Miesch, C.; Boldo, D.; Briotte, X.; Valorge, C.; Le Men, H. (2008): ICARE: A physically-based model to correct atmospheric and geometric effects from high spatial and spectral remote sensing images over 3D urban areas. Meteorology and Atmospheric Physics, vol. 102, pp. 209-222.

Li, X.; Guo, H.; Sun, Z.; Shen, G. (2011): Urban Impervious Surfaces Estimation from RADARSAT-2 Polarimetric Data Using SVM Method. PIERS ONLINE, vol. 7, no. 7, 2011, pp. 671-676.

Marconcini, M., Esch, T., Felbier, A., Heldens, W. (2013): High-Resolution Global Monitoring of Urban Settlements. Proceedings of the RealCORP2013 Conference, 20-23 May 2013, Rome.

Mende, A.; Heiden, U.; Bachmann, M.; Hoja, D.; Buchroithner, M. (2011): Development of a new spectral library classifier for airborne hyperspectral images on heterogeneous environments. Proceedings of the 7th EARSeL Workshop of the Special Interest Group in Imaging Spectroscopy, 11-13 April 2011, Edinburgh, Scotland.

Meister, G.; Rothkirch, A.; Wiemker, R.; Bienlein, J.; Spitzer, H. (1998): Modeling the directional reflectance (BRDF) of a corrugated roof and experimental verification. Proceedings of IGARSS 1998, 6-10 July 1998, Seattle, WA, USA.

Meister, G.; Rothkirch, A.; Spitzer, H.; Bienlein, J.K. (2001): Large-scale bidirectional reflectance model for urban areas. IEEE Transactions on Geoscience and Remote Sensing, vol. 39, pp. 1927-1942.

NASA (2012): http://hyspiri.jpl.nasa.gov/downloads/2012_Workshop/day3/4_Matsunaga_HISUI_Status.pdf, 20/07/13.

NASA (2013a): http://modis.gsfc.nasa.gov/, 20/07/13.

NASA (2013b): http://landsat.gsfc.nasa.gov/, 20/07/13.

NASA (2013c): http://hyspiri.jpl.nasa.gov/, 20/07/13.

Niu, X.; Ban, Y. (2010): Multitemporal RADARSAT-2 polarimetric SAR data for urban land-cover mapping. Proceedings of ISPRS Technical Commission VII Symposium 2010, pp. 175-180.

NOAA (2013a): http://ngdc.noaa.gov/eog/dmsp.html, 20/07/13.

NOAA (2013b): http://www2.ncdc.noaa.gov/docs/klm/html/c3/sec3-1.htm, 20/07/13.

Palubinskas, G.; Reinartz, P. (2011): Multi-resolution, multi-sensor image fusion: general fusion framework. Proc. of Joint Urban Remote Sensing Event JURSE, 11-13 April, Munich, Germany (in print).

Potere, D.; Schneider, A.; Angel, S.; Civco, D.L. (2009) Mapping urban areas on a global scale: which of the eight maps now available is more accurate? International Journal of Remote Sensing, vol. 30, pp. 6531-6558.

Powell, R.L.; Roberts, D.A.; Dennison, P.E.; Hess, L.L. (2007): Sub-pixel mapping of urban land cover using multiple endmember spectral mixture analysis: Manaus, Brazil. Remote Sensing of Environment, vol. 106, pp. 253-267.

RapidEye (2013): http://www.rapideye.com/products/index.htm, 20/07/13.

Rashed, T.; Jürgens, C. (2010): Remote Sensing of Urban and Suburban Areas. Springer.

Richter, R.; Müller, A. (2005): De-shadowing of satellite/airborne imagery. International Journal of Remote Sensing, vol. 26, pp. 3137-3148.

Schneider, A.; Friedl, M.A.; Potere, D. (2010): Mapping global urban areas using MODIS 500-m data: New methods and datasets based on 'urban ecoregions'. Remote Sensing of Environment, vol. 114, pp. 1733-1746.

Small, C. (2001): Estimation of urban vegetation abundance by spectral mixture analysis. International Journal of Remote Sensing, vol. 22, pp. 1305-1334.

Strozzi, T.; Dammert, P.; Wegmüller, U.; Martinez, J.-M.; Askne, J.; Beaudoin, A.; Hallikainen, M. (2000): Landuse mapping with ERS SAR interferometry. IEEE Trans. Geosci. Remote Sensing, vol. 38, pp. 766-775.

Taubenböck, H.; Goseberg, N.; Setiadi, N.; Lämmel, G.; Moder, F.; Oczipka, M.; Klüpfel, H.; Wahl, R.; Schlurmann, T.; Strunz, G.; Birkmann, J.; Nagel, K.; Siegert, F.; Lehmann, F.; Dech, S.; Gress, A.; Klein, R. (2009): Last-Mile preparation for a potential disaster - Interdisciplinary approach towards tsunami early warning and an evacuation information system for the coastal city of Padang, Indonesia. In: Nat. Hazards and Earth Sys. Sci., vol. 9, pp. 1509-1528.

Taubenböck, H.; Esch, T.; Wurm, M.; Roth, A.; Dech, S. (2010a): Object-based feature extraction using high spatial resolution satellite data of urban areas. Journal of Spatial Science, vol. 55, no. 1, pp. 117-133.

Taubenböck, H.; Wegman, M.; Wurm, M.; Ullmann, T.; Dech, S. (2010b): The global trend of urbanization - Spatiotemporal analysis of mega cities using multi-temporal remote sensing, landscape metrics and gradient analysis. SPIE's International Symposium, Remote Sensing Europe, 20-23 September, Toulouse, France.

Taubenböck, H.; Esch, T.; Felbier, A.; Wiesner, M.; Roth, A.; Dech, S. (2012a): Monitoring of mega cities from space. In: Remote Sensing of Environment, vol. 117, pp. 162-176.

Taubenböck, H.; Felbier, A.; Esch, T.; Roth, A.; Dech, S. (2012b): Pixel-based classification algorithm for mapping urban footprints from radar data - a case study for RADARSAT-2. In: Can. J. Remote Sensing, vol. 38, no. 3, pp. 211-222.

UGS (2013): http://www.cosmo-skymed.it/en/index.htm, 20/07/13.

UNDP (2013): "United Nations Department of Economic and Social Affairs-Population Division," World Urbanization Prospects: The 2007, Revision, CD-ROM (2008).

Ungar, S.G.; Reuter, D.; Pearlman, J.S.; Mendenhall, J.A. (2003): Overview of the Earth Observing One (EO-1) mission. IEEE Transactions on Geoscience and Remote Sensing, vol. 41, pp. 1149-1159.

Wang, Y.; Zhu, X.; Bamler, R.; Gernhardt, S. (2013): Towards TerraSAR-X Street View: Creating City Point Cloud from Multi-aspect Data Stacks. Proc. of Joint Urban Remote Sensing Event, JURSE 2013, Sao Paolo, Brazil,

Weng, Q.; Hu, X.; Lu, D. (2008): Extracting impervious surfaces from medium spatial resolution multispectral and hyperspectral imagery: a comparison. International Journal of Remote Sensing, vol. 29, pp. 3209-3232.

Weng, Q.; Quattrochi, A.; Carlson, T. (2012): Remote Sensing of Urban Environments. In: Remote Sensing of Environment.
http://www.sciencedirect.com/science/publication?issn=00344257&volume=117, 03/07/2013.

Weydahl, D.J. (2001): Analysis of ERS SAR coherence images acquired over vegetated areas and urban features. International Journal of Remote Sensing, vol. 22, no. 14, pp. 2811-2830.

Xu, B.; Gong, P. (2007): Land-use/Land-cover classification with multispectral and hyperspectral EO-1 data. Photogrammetric Engineering and Remote Sensing, pp. 955-965.

Xu, W.; Wooster, M.; Grimmond, C. (2008): Modelling of urban sensible heat flux at multiple spatial scales: A demonstration using airborne hyperspectral imagery of Shanghai and a temperature emissivity separation approach. Remote Sensing of Environment, vol. 112, pp. 3493-3510.

Yang, X. (2011): Urban Remote Sensing: Monitoring, Synthesis and Modeling in the Urban Environment. Wiley-Blackwell. ISBN: 978-0-470-74958-6, p. 408.

Zhang, J. (2010): Multi-source remote sensing data fusion: status and trends. International Journal of Image and Data Fusion, vol. 1, pp. 5-24.